

A density-functional and molecular-dynamics study on the physical properties of yttrium-doped tantalum oxynitride

H. Wolff^a, H. Schilling^b, M. Lerch^b, R. Dronskowski^{a,*}

^a*Institut für Anorganische Chemie, RWTH Aachen, Landoltweg 1, 52056 Aachen, Germany*

^b*Institut für Chemie, TU Berlin, Straße des 17. Juni 135, 10623 Berlin, Germany*

Received 19 December 2005; received in revised form 25 January 2006; accepted 28 January 2006

Available online 28 February 2006

Dedicated to Professor Hans-Georg von Schnering on the occasion of his 75th birthday

Abstract

Fluorite-type phases in the system Y–Ta–O–N have been studied using both first-principle electronic-structure calculations and molecular-dynamic simulations to validate the structural data and to explain unusual asymmetric reflection profiles observed in the experimental X-ray diffraction patterns. We provide evidence that the compounds may be macroscopically described as to represent cubic fluorite-type defect structures despite the fact that DFT calculations clearly show that all crystallographic unit cells appear as triclinically distorted. Additionally, we find that there is a minute (but hardly significant) tendency for anionic ordering at absolute zero temperature but none under reaction conditions.

© 2006 Elsevier Inc. All rights reserved.

Keywords: Oxynitrides; Crystal structure; Ionic ordering; Density-functional theory; Molecular-dynamic simulations

1. Introduction

In the field of solid-state materials research, the phases dubbed *oxynitrides* have recently attracted increased interest [1–4]. Oxynitrides are easily accessible from metal oxides and ammonia [5] and, moreover, their properties can be stoichiometrically tuned via the amount of nitrogen incorporated [6]. One of the most exciting properties of these phases is given by their color, which makes oxynitrides promising candidates for replacing conventional pigments usually containing heavy (and potentially toxic) metals [1]. It turns out that, among the many synthetic candidates, rare-earth- or yttrium-doped tantalum oxynitride appears as especially suitable for that purpose. In addition, it is well known that the corresponding doped oxides show luminescence under ultraviolet light

[7], and the luminescence may be shifted into the visual region simply by nitridation [8].

Since TaON is one of the very few oxynitrides with an ordered O/N arrangement [9], the question arises whether the doped derivatives also exhibit an ordered anionic distribution. Alternatively, a fully (or partially) random-like O/N arrangement is thinkable, as indicated from neutron diffraction experiments [10].

The aim of the present work is to theoretically characterize fluorite-type phases of TaON, stabilized by doping with Y₂O₃, which appear as being cubic at first sight. In order to augment the fundamental experimental studies [11], computational chemistry was believed to allow for a better understanding of the structural properties as deduced from the experimentally observed diffraction data. Density-functional theory (DFT) appears to be a fine instrument for investigations on doped TaON, for it has been successfully utilized in former studies on the pure TaON phase [12–15]. In addition, molecular dynamic (MD) simulations were carried out on structures that had been optimized using quantum-mechanical

*Corresponding author. Fax: +49 241 80 92642.

E-mail address: drons@HAL9000.ac.rwth-aachen.de
(R. Dronskowski).

schemes, such as to move away from absolute zero temperature.

2. Synthesis

As precursors, amorphous ternary phases in the system Y–Ta–O were prepared using a modified Peccini method. Tantalum chloride (Alfa Aesar, 99.99%) was solved in ethanol containing citric acid in an excess of 12 times the amount of TaCl₅. The possibly occurring dispersed Ta₂O₅ can be removed by centrifugation. The resulting tantalum citrate complexes are insensitive to water. A stock solution with a defined content of tantalum citrate was obtained. Yttrium oxide (Alfa Aesar, 99.99%) was solved under heating in a small volume of hydrochloric acid. This YCl₃ solution was poured into ethanol containing citric acid in an excess of 12 times the amount of YCl₃. Appropriate quantities of the two citrate solutions were mixed together, and ethylene glycol in an excess of 17 times the metals content was added. The solvent and HCl were evaporated, and the citrate complexes together with ethylene glycol were polymerized at about 150 °C. The organic residues of the polymer were burnt off at 600 °C for 16 h to give white amorphous powders. These oxides were treated under ammonia at temperatures between 700 and 1000 °C for 16 h with a flow rate of 20 l/h.

3. Theory

Density-functional total-energy calculations were performed with the Vienna ab-initio Simulation Package (VASP) that has been developed at the Institut für Theoretische Physik of the Technische Universität Wien [16,17]. The valence electrons were handled by ultrasoft pseudopotentials of Vanderbilt type [18] while the Kohn–Sham orbitals were expanded from a plane wave basis set with a kinetic cutoff of 490 eV. Correlation and exchange terms between the electrons were factored in by the GGA functional of Perdew and Wang [19]. The Brillouin zone was sampled using 128 irreducible *k* points as they resolve from a 4 × 8 × 8 Monkhorst–Pack grid and, for larger supercells, 16 irreducible *k* points from a 4 × 4 × 4 mesh, respectively. Both structural and electronic relaxations were performed, starting with structural parameters that were obtained from X-ray diffraction (XRD) [11] as summarized in Table 1. Eventually, the total energies were calculated for different cell volumes and fitted to the

Birch–Murnaghan equation of state

$$E(V) = \frac{9B_0V_0}{16} \left[(B'_0 - 4) \left(\frac{V_0}{V} \right)^2 + (14 - 3B'_0) \left(\frac{V_0}{V} \right)^{4/3} + (3B'_0 - 16) \left(\frac{V_0}{V} \right)^{2/3} \right] + \left(E(V_0) - \frac{9B_0V_0}{16}(B'_0 - 6) \right) \quad (1)$$

to obtain access to equilibrium energies and volumes, E_0 and V_0 , as well as to the bulk moduli B_0 .

MD simulations were carried out with the aixCCAD code [20,21], which has been developed at our own institute at RWTH Aachen on the basis of the bond-valence method. The necessary r_0 parameters for the Ta–O, Ta–N, Y–O and Y–N combinations are 1.920, 2.010, 2.014 and 2.170 Å, and they were taken from the tabulation of Brese and O’Keeffe [22]. The final simulation boxes consisted of about 900 atoms, the total number somewhat depending on the stoichiometry of the compound under question. Applying a temperature of 300 K, simulations were executed over a total of 200 000 steps of 0.001 fs each.

To theoretically simulate diffractive data, the crystal coordinates obtained from the MD simulations were first imported into the program ATOMS 6.2. Second, the *whole* simulation box was considered as *one* very large crystallographic unit cell without any symmetry restrictions (space group *P1*). The diffraction patterns were then calculated for Cu $K\alpha$ radiation ($\lambda = 1.5418$ Å).

4. Results and discussion

4.1. Structural model

In order to build a reasonable structural model to be used by the computational methods, a good starting point is given by the averaged structural information as derived from the experimental X-ray powder diffraction pattern of Y_{0.15}Ta_{0.85}O_{0.62}N_{1.15} listed in Table 1.

Assuming a (hypothetic) cubic phase of TaON at the outset, this minimum unit cell was doubled in size along one lattice vector, leading to an enlarged unit cell (or simulation box) containing a total of 24 atoms. To realize different amounts of dopant in the theoretical description, a maximum of four tantalum atoms were replaced, one after another, by yttrium atoms and, to maintain

Table 1
Structural data of Y_{0.15}Ta_{0.85}O_{0.62}N_{1.15} derived from X-ray powder diffraction [11], used as starting parameters for structural relaxation

Structure type	Fluorite	Atom	Site	<i>x</i>	<i>y</i>	<i>z</i>	Occ.
Space group	<i>Fm</i> $\bar{3}$ <i>m</i>	Y	4 <i>a</i>	0	0	0	0.15
<i>a</i> (Å)	5.0855(2)	Ta	4 <i>a</i>	0	0	0	0.85
<i>V</i> (Å ³)	131.52	O	8 <i>c</i>	$\frac{1}{4}$	$\frac{1}{4}$	$\frac{1}{4}$	0.31
<i>Z</i>	4	N	8 <i>c</i>	$\frac{1}{4}$	$\frac{1}{4}$	$\frac{1}{4}$	0.58

electroneutrality, up to three anion vacancies were introduced into the simulation box. This yields four theoretical model systems dubbed $Y_nTa_{1-n}O_xN_y$ covering a stoichiometric range of $0.125 \leq n \leq 0.5$.

4.2. Ionic ordering

The first problem to theoretically clarify is given by the (potential) anionic ordering in stoichiometrically exact $Y_{0.5}Ta_{0.5}O_{0.875}N_{0.75}\square_{0.375}$ adopting the fluorite crystal structure. Among the many possibilities for placing the anions around the cations, there are three which are worth taking a closer look at. For example, one may think of a homogeneous anionic environment around *all* the cationic sites, as it is realized by parallel layers of the different anions (Fig. 1, type I) or an alternating arrangement of nitrogen and oxygen (Fig. 1, type II). Alternatively, it is also possible to put the oxide ions around the lower-valent Y dopant cation, as it was done in Fig. 1, type III.

Note that, in the fluorite structure, all anions are tetrahedrally coordinated by four cations charged q_i and the cations experience cubic coordination by eight anions charged q_j . The opposing (formal) charge for each anionic site is then $\sum_i^4 q_i/8$, and for each anionic site it is given by $\sum_j^8 q_j/4$. Using this extremely simple electrostatic model

one might anticipate already that the permutations I or II will be preferred in oxynitrides with a high Ta^{5+} amount, because all cationic sites are then opposed with a formal charge of $4 \times (-2/4) + 4 \times (-3/4) = -5$, thereby yielding the highest Madelung energy. Arrangement III, however, is the better choice for Y^{3+} -rich derivatives, for half of the yttrium cations experience an opposite charge of $8 \times (-2/4) = -4$ due to their coordination by eight oxygen anions. Not too surprisingly, this is exactly what we find in the total-energy calculations, as can be seen in Table 2 and, furthermore, in Fig. 2.

As is obvious from Table 2, the differences in energy are only small for a low yttrium content. Upon increasing the amount of dopant, the total energy becomes more dependent on the ionic distribution, favoring the ordered variant III.

Given the knowledge which of the *ordered* structures is the most favorable, we still have to determine the relative stability of a fully *disordered* one. To do so, we chose to calculate a supercell that was quadrupled in size and represented a statistical distribution of the anions. To make sure that we came close to a fully disordered anionic setting, we then performed calculations for three alternative and seemingly disordered geometries, resulting in a total-energy difference of merely ± 0.1 eV. Given the

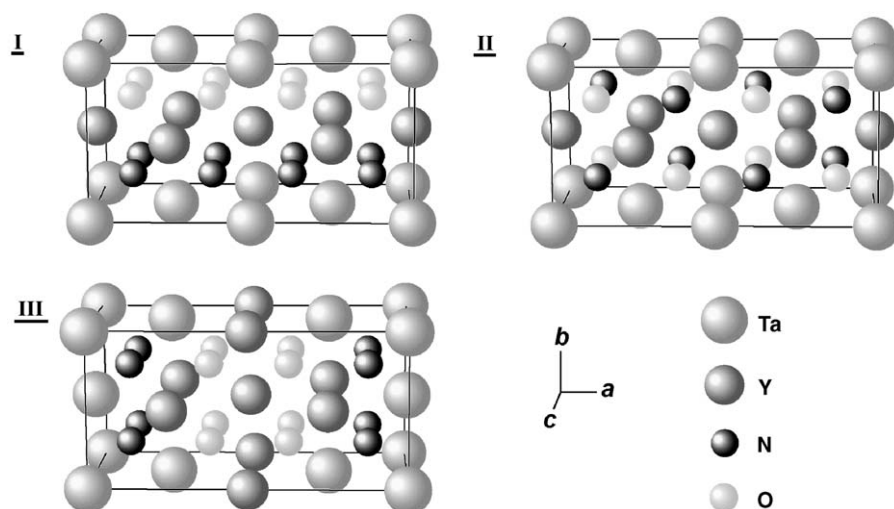


Fig. 1. Three possible ways of ion ordering in $Y_{0.5}Ta_{0.5}O_{0.875}N_{0.75}$: parallel layers (I), alternating anions (II), oxygens clustered around yttrium (III). For simplicity, anion vacancies are not shown in this figure.

Table 2

Equilibrium energies and volumes per formula unit of three ordered fluorite-type structures (I, II, III) of doped TaON as well as one disordered variant (IV)

	E_0 (eV)				V_0 (\AA^3)			
	I	II	III	IV	I	II	III	IV
$Y_{0.125}Ta_{0.875}O_{0.875}N_{0.125}\square_{0.125}$	-29.10	-29.09	-29.03	-29.06	-33.46	-34.74	-32.47	-32.94
$Y_{0.25}Ta_{0.75}O_{0.75}N_{0.25}\square_{0.25}$	-27.79	-27.78	—	—	-35.74	-33.04	—	—
$Y_{0.375}Ta_{0.625}ON_{0.75}\square_{0.25}$	-27.13	-26.95	-26.97	—	-35.14	-33.95	-34.45	—
$Y_{0.5}Ta_{0.5}O_{0.875}N_{0.75}\square_{0.375}$	-25.42	-25.59	-25.72	—	-34.55	-35.10	-36.34	—

limited accuracy of the computational approach, all three calculated disordered structural models are energetically comparable. Upon comparing these three with the lowest-energy *ordered* variant, as it is done in Fig. 3, it is clear that full anion ordering does lead to a further energetic stabilization, but the energy gain (ca. 0.04 eV or 3.9 kJ/mol) is so tiny that the notion of a structurally fully ordered ground state is an oversimplification, even at absolute zero temperature. Moreover, under synthesis conditions of about 1000 K, the entropical term $T\Delta S$ has

to be taken into account because, upon interchange of O and N, the mixing entropy S_{con} increases. If, as it has been done in former contributions on related systems such as Zr_2ON_2 [23] or $\text{Si}_2\text{N}_2\text{O}$ [24], the mixing entropy S_{con} is estimated with the simple formula

$$S_{\text{con}} = R \sum_i x_i \ln x_i, \quad (2)$$

with R being the ideal gas constant and x_i the molar fraction of the anion i , an energetic gain of $T\Delta S_{\text{con}} = 5.7 \text{ kJ/mol}$ results purely because of structural disorder. Thus, the aforementioned small preference for anionic ordering no longer exists, and the experimentally obtained compounds can be predicted to exhibit fully *random* anionic distribution because of the high temperatures upon synthesis.

4.3. Calculated structural data

In Table 3 we list the structural parameters for the increasingly doped tantalum oxynitrides, and these numerical entries have been extracted from the energy minima found in the calculations achieving full structural relaxation (see Fig. 4). While there exists a stable cubic structure for undoped TaON, doping leads to a considerable distortion of the fluorite-type structures. Besides such triclinic distortion, a steady increase in the cell volume is also observed with growing dopant amount.

The symmetry lowering also shows up in the local environment of the individual atoms, expressed by their

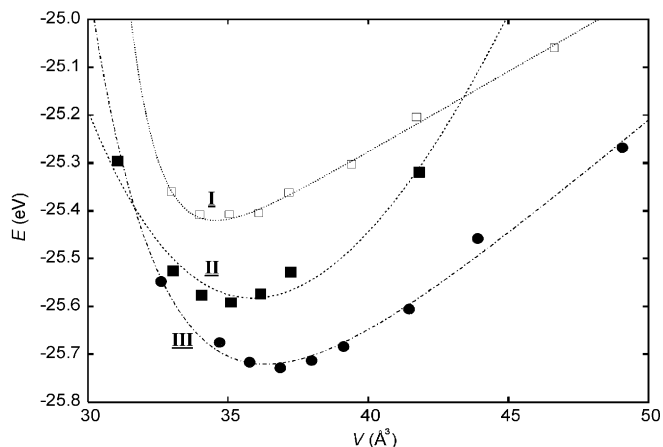


Fig. 2. Energy and volume per formula unit for ordering variants I, II and III (see also Fig. 1) in $\text{Y}_{0.5}\text{Ta}_{0.5}\text{O}_{0.875}\text{N}_{0.25}\square_{0.375}$.

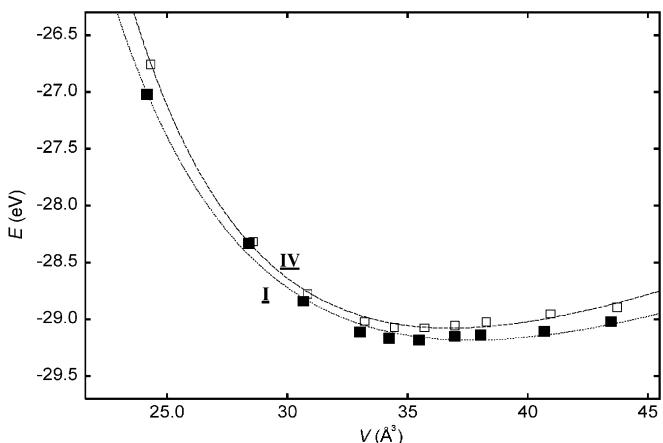


Fig. 3. Energy and cell volume per formula unit of $\text{Y}_{0.125}\text{Ta}_{0.875}\text{O}_{0.875}\text{N}\square_{0.125}$ in ordering variant I and for a statistical ion distribution (IV) within a simulation box quadrupled in size.

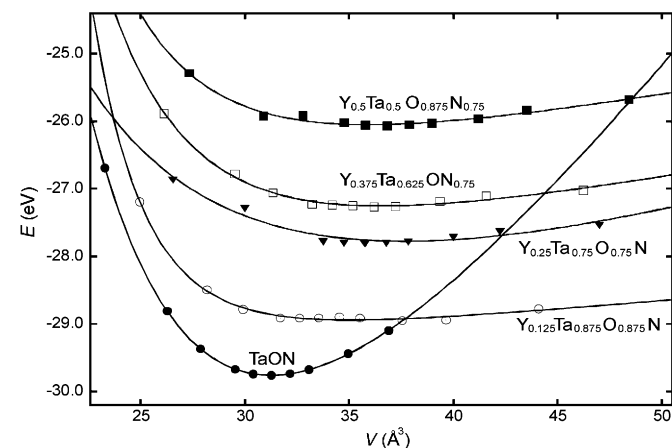


Fig. 4. Energy and volume per formula unit for increasingly doped TaON.

Table 3

Calculated structural and physical data of the (pseudo)-cubic unit cells

	a (Å)	b (Å)	c (Å)	α (deg)	β (deg)	γ (deg)	V_0 (Å ³)	B_0 (GPa)
TaON	4.99	4.99	4.98	90.0	90.0	90.0	124.04	299 ± 0.3
$\text{Y}_{0.125}\text{Ta}_{0.875}\text{O}_{0.875}\text{N}\square_{0.125}$	5.16	5.19	5.03	94.8	91.9	86.3	139.96	70 ± 10
$\text{Y}_{0.25}\text{Ta}_{0.75}\text{O}_{0.75}\text{N}\square_{0.25}$	5.25	5.23	5.34	90.0	76.9	90.0	150.88	62 ± 13
$\text{Y}_{0.375}\text{Ta}_{0.625}\text{ON}_{0.75}\square_{0.25}$	5.00	5.30	5.31	87.7	89.5	93.0	146.20	66 ± 5
$\text{Y}_{0.5}\text{Ta}_{0.5}\text{O}_{0.875}\text{N}_{0.75}\square_{0.375}$	5.00	5.40	5.48	93.8	90.5	87.4	145.32	64 ± 6

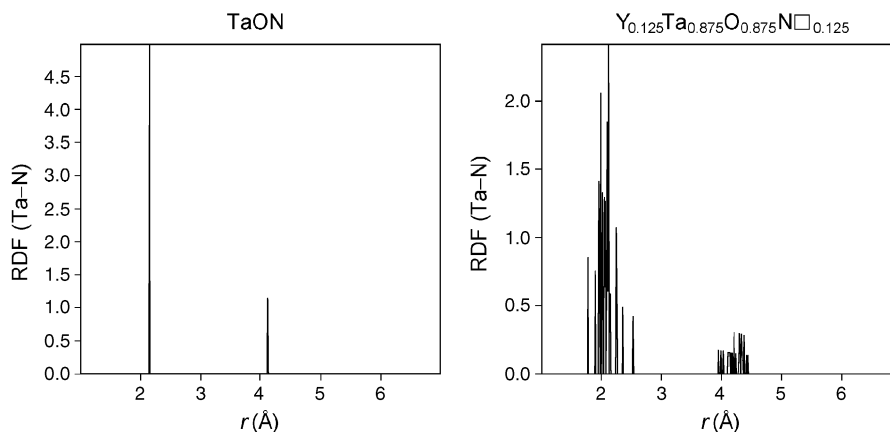


Fig. 5. Radial distribution of nitrogen around tantalum in undoped cubic TaON (left) and in $Y_{0.125}Ta_{0.875}O_{0.875}N_{0.125}$, respectively (right).

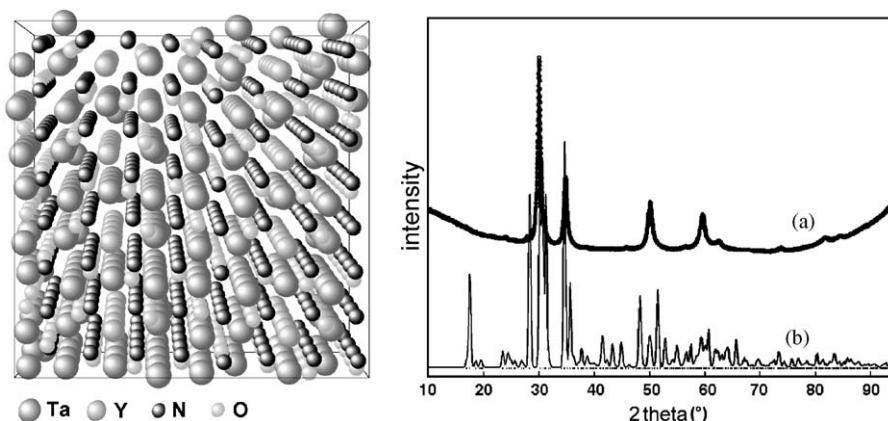


Fig. 6. Supercell with structural parameters from DFT calculations (left) and XRD patterns (right): experimental pattern (a) of $Y_{0.15}Ta_{0.85}O_{0.62}N_{1.15}$ and simulated pattern (b) for $Y_{0.125}Ta_{0.875}O_{0.875}N_{0.125}$, which is the supercell on the left.

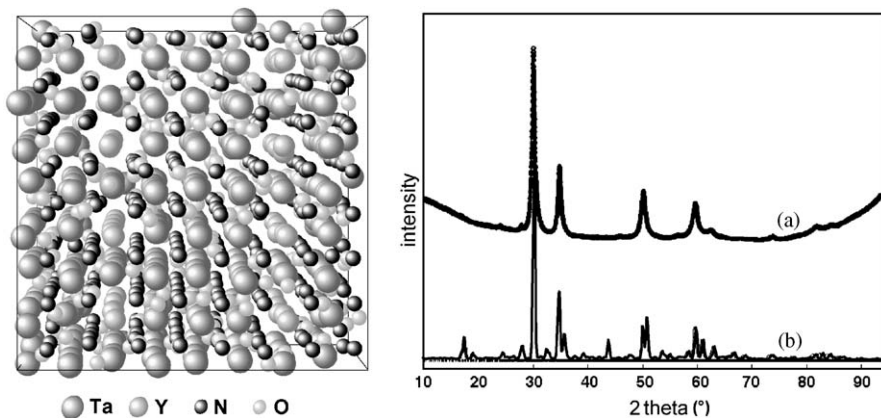


Fig. 7. Same as in Fig. 6, but after an MD simulation at 300 K; also see text.

radial distribution functions (RDF). The RDF of the Ta–N pair (Fig. 5), for example, clearly shows that in the structures of the doped oxynitrides, the presence of *defects* makes the anions move away from their crystallographic high-symmetry sites in favor of an optimized charge

distribution, leading to a decrease in packing density and, thus, to lattice expansion.

Because of that increased spacing, the stiffness of the yttrium-containing compounds is low if compared with the pure TaON phase, which can be seen from the flattened

E/V -curves in Fig. 4. Such non-ideal (i.e., defect-containing) solid materials obviously do not fit the Birch–Murnaghan equation of state very well, and the calculated bulk moduli in Table 3 allow only a rough numerical estimate of the magnitude. The undoped cubic phase's bulk modulus, however, can be easily determined to 299 GPa, which is close to the one of β -TaON (278 GPa) [12].

4.4. Simulation of diffraction patterns

Because of the small deviations of the individual ions from their ideal lattice sites, structural determination via XRD becomes a difficult task, for it leads to *broad, asymmetric* reflection profiles [11]. Although it is still possible to describe yttrium-doped tantalum oxynitrides as *cubic* structures of a defect-fluorite type, such a description involves the introduction of empirical correction factors (such as “strain” parameters) to eventually fit the aforementioned asymmetric reflection profiles. Not too surprisingly, quantum-chemical total-energy calculations evidence triclinic distortions of the fluorite-type minimum unit cells in *all* cases, somewhat depending on the individual compositions. Thus, a simulated XRD pattern (Fig. 6), which can be generated on the basis of the quantum-chemically calculated structural data, shows considerable differences from the experimental one.

This simple model for $T = 0$ K, however, can be significantly improved by assuming that any macroscopic probe may be looked upon as an ensemble of a vast multiplicity of individually distorted “unit cells” with likewise statistically distributed structural distortions [11]. Such a physical description may be nicely modelled by classical MD simulation of a sufficiently large supercell based on the calculated structural parameters. After relaxation at 300 K, thereby moving away from absolute zero temperature and allowing the atoms to get closer to the thermal average, the supercell and its geometry may be utilized to generate an XRD pattern. The latter appears in good agreement with that of the real “cubic” compound (Fig. 7) despite the fact that the local symmetry is no longer cubic.

5. Conclusions

First-principle calculations and classical MD simulations were performed for yttrium-doped tantalum oxynitride. The classification of these compounds as being of a defect-fluorite type is justified from the macroscopic point of view, as evidenced from simulated XRD patterns of thermally averaged supercells. Microscopically, DFT calculations clearly show that the crystallographic unit cells are triclinically distorted because the anions shift towards vacant lattice sites. At the same time, the large number of

structural defects is responsible for the exceptionally low bulk moduli.

Regarding ionic ordering, we have shown that, at absolute zero temperature, there is a minute (but hardly significant) preference for those ordered permutations which lead to an optimum in charge distribution. At synthesis conditions, however, this effect is offset by the mixing entropy, such that the real material may be safely looked upon as entirely disordered in terms of the O/N atoms.

Acknowledgments

The authors wish to thank the computing centers at RWTH Aachen University and Jülich Research Center for providing large amounts of CPU time. This work is supported by Deutsche Forschungsgemeinschaft within priority program 1136.

References

- [1] M. Jansen, H.P. Litschert, *Nature* 404 (2000) 980.
- [2] G. Hitoki, T. Takata, J.N. Kondo, M. Hara, H. Kobayashi, K. Domen, *Chem. Commun.* (2002) 1698.
- [3] K. Miga, K. Stanczyk, C. Sayag, D. Brodzki, G. Djéga-Mariadassou, *J. Catal.* 183 (1999) 63.
- [4] Y.-I. Kim, P.M. Woodward, K.Y. Baba-Kishi, C.W. Tai, *Chem. Mater.* 16 (2004) 1267.
- [5] R. Marchand, Y. Laurent, J. Guyader, P. l'Haridon, P. Verdier, *J. Eur. Ceram. Soc.* 8 (1991) 197.
- [6] R. Marchand, *CR Acad. Sci. Paris IIc* 2 (1999) 667.
- [7] G. Blasse, A. Bril, *J. Lumin.* 3 (1970) 109.
- [8] F. Tessier, R. Marchand, *J. Solid State Chem.* 171 (2003) 143.
- [9] D. Armytage, B.E.F. Fender, *Acta Crystallogr. B* 30 (1974) 809.
- [10] P. Maillard, F. Tessier, E. Orhan, F. Cheviré, R. Marchand, *Chem. Mater.* 17 (2005) 152.
- [11] H. Schilling, H. Wolff, R. Dronskowski, M. Lerch, *Z. Naturforsch. B*, in press.
- [12] C.M. Fang, E. Orhan, G.A. de Wijs, H.T. Hintzen, R.A. de Groot, R. Marchand, J.-Y. Saillard, G. de With, *J. Mater. Chem.* 11 (2001) 1248.
- [13] C.M. Fang, R. Metselaar, H.T. Hintzen, G. de With, *Key Eng. Mater.* 206–213 (2002) 1149.
- [14] M.-W. Lumey, R. Dronskowski, *Z. Anorg. Allg. Chem.* 623 (2003) 2173.
- [15] T. Bredow, M.-W. Lumey, R. Dronskowski, H. Schilling, J. Pickardt, M. Lerch, *Z. Anorg. Allg. Chem.*, in press.
- [16] G. Kresse, J. Furthmüller, *Comp. Mater. Sci.* 6 (1996) 15.
- [17] G. Kresse, J. Furthmüller, *Phys. Rev. B* 54 (1996) 11169.
- [18] D. Vanderbilt, *Phys. Rev. B* 41 (1990) 7892.
- [19] J.P. Perdew, in: *Electronic Structure of Solids '91*, Akademie Verlag, Berlin, 1991.
- [20] B. Eck, R. Dronskowski, *J. Alloys Compd.* 338 (2002) 136.
- [21] B. Eck, Y. Kurtulus, W. Offermanns, R. Dronskowski, *J. Alloys Compd.* 338 (2002) 142.
- [22] N.E. Brese, M. O'Keeffe, *Acta Crystallogr. B* 47 (1991) 192.
- [23] T. Bredow, M. Lerch, *Z. Anorg. Allg. Chem.* 630 (2004) 2262.
- [24] P. Kroll, M. Milko, *Z. Anorg. Allg. Chem.* 629 (2003) 1737.